coatings

MDPI

Article

Studies of New Layer Formation on the Surface of Zinc Doped Hydroxyapatite/Chitosan Composite Coatings in Biological Medium

Mikael Motelica-Heino [1], Mihai Valentin Predoi [2], Steluta Carmen Ciobanu [3], Simona Liliana Iconaru [3,*] and Daniela Predoi [3,*]

[1] Department of Civil Engineering and Environment, Université d'Orléans, ISTO, UMR 7327 CNRS, 1A Rue de la Férollerie, 45071 Orléans, France
[2] Department of Mechanics, University Politehnica of Bucharest, BN 002, 313 Splaiul Independentei, Sector 6, 060042 Bucharest, Romania
[3] National Institute of Materials Physics, Atomistilor Street, No. 405A, P.O. Box MG 07, 077125 Magurele, Romania
* Correspondence: simonaiconaru@gmail.com (S.L.I.); dpredoi@gmail.com (D.P.)

Abstract: Usually, before being used in biomedical applications, a biomaterials' bioactivity is tested by *in vitro* methods that simulate similar conditions to those found in the human body. In this work, we report on the synthesis of zinc-doped hydroxyapatite–chitosan (ZnHApC) composite coatings by the vacuum deposition method. The surface microstructure and the chemical and molecular modification of the coatings before and after soaking in DMEM (Dulbecco's Modified Eagle's Medium) were studied. For this objective, techniques such as attenuated total reflection (ATR), Fourier transform infrared (FTIR) spectroscopy, metallographic microscopy (MM), and scanning electron microscopy (SEM) were applied used. Also, water contact angle measurements and swelling studies were made on ZnHApC composite coatings before and after soaking in a biological medium. The coatings' adherence to the substrate was also studied. The results of antifungal studies on ZnHApC composite coatings against the *Candida albicans* microbial strain reveal their good antifungal activity. The biocompatibility of the composite coatings was tested using a primary osteoblast cell line. Our results suggest that zinc-doped hydroxyapatite–chitosan samples could be used as a bioimplant material due to their enhanced bioactivity and biocompatibility.

Keywords: biological medium; zinc; surface changes; hydroxyapatite; osteoblast cell line

check for updates

Citation: Motelica-Heino, M.; Predoi, M.V.; Ciobanu, S.C.; Iconaru, S.L.; Predoi, D. Studies of New Layer Formation on the Surface of Zinc Doped Hydroxyapatite/Chitosan Composite Coatings in Biological Medium. *Coatings* **2023**, *13*, 472. https://doi.org/10.3390/coatings13020472

Academic Editor: Seungil Kim

Received: 31 December 2022
Revised: 10 February 2023
Accepted: 17 February 2023
Published: 19 February 2023

Copyright: © 2023 by the authors. Licensee MDPI, Basel, Switzerland. This article is an open access article distributed under the terms and conditions of the Creative Commons Attribution (CC BY) license (https://creativecommons.org/licenses/by/4.0/).

1. Introduction

Usually, prior to being used in biomedical applications (e.g., coatings for medical devices, metallic implants, bone fillers, etc.), biomaterials are tested for their bioactivity through *in vitro* methods that simulate similar conditions to those found in the human body [1]. For this purpose, since the beginning of the 1990s, SBF (simulated body fluid) was proposed by Kokubo et al. as a medium that could predict the in vivo bone bioactivity of a biomaterial [2]. Normally, the SBF solution contains only the inorganic part of blood serum [3,4].

Recently, in the literature, it was proposed to use DMEM (Dulbecco's Modified Eagle's Medium) solution as a substitute for SBF solution in order to evaluate a material's bioactivity [1,4]. DMEM solution is frequently used as a culture medium for cell lines, and, unlike SBF, contains both the inorganic and the organic parts of blood serum [1,4]. In previous studies, it has been highlighted that by immersing samples in SBF or DMEM solution (between 1 and 21 days), the precipitation of an apatitic layer on the sample surface occurs [4–6]. It is well known that the formation of new bone tissue around the implant implies many biological processes that take place at the interface between the implant and

the bone tissue [6]. Hydroxyapatite (HAp) is one of the most often used biomaterials for covering metallic implants [6,7].

Among the most common causes that lead to implant failure are infections that occur immediately after the implant and the formation of an insufficient amount of new bone tissue around the implant [8]. Furthermore, previous studies have shown that the bioactivity of hydroxyapatite layers can be improved by ionic substitution [8,9]. For example, in the study conducted by Kazimierczak P. et al. [10] regarding the biocompatibility and osteoinductivity of chitosan–agarose–nanohydroxyapatite scaffolds, it was reported that the hydrophilic surface of the obtained nanocomposites confers on them a good biocompatibility with the osteoblast (hFOB 1.19) cell line. Furthermore, the presence of zinc ions in the zinc-doped nanohydroxyapatite-based bone scaffolds gives them excellent antimicrobial properties and a nontoxic effect against the osteoblast cell line [11].

On the other hand, *Candida* species are well known as an important nosocomial pathogen. Moreover, *Candida albicans* is frequently identified in the biofilm found on the surface of implanted biomedical devices (e.g., urinary catheters, joint replacements, etc.) [12–14]. Therefore, the attainment of biomaterials with good antifungal activity is of great interest to the medical community and could represent a viable alternative to the classic antimycotic treatment.

Currently, for the development of bioceramic layers, techniques such as electrophoretic deposition [15], pulsed laser deposition (PLD) [16], matrix-assisted pulsed laser deposition (MAPLE) [17], radio frequency magnetron sputtering (RFMS) [18], the sol-gel method [19], electrochemical deposition [20], vacuum deposition [21], etc., are used.

For example, Vranceanu D. M. et al. [6] have found, along with the growth of the immersion time (up to 21 days) of silver-doped hydroxyapatite (AgHAp) and hydroxyapatite (HAp) coatings in a DMEM solution, the formation of increased quantities of new apatite phases on their surface [6]. This behavior suggests that the studied samples have an improved biomineralization ability [6]. The results obtained on the AgHAp and HAp coatings after immersion in an SBF solution were discussed. Their results indicate that the DMEM solution may be used for preliminary evaluation of biomineralization efficiency [6].

Another study, conducted by Dumelie N. and collaborators [22] revealed that after the immersion of up to 21 days in a DMEM medium of calcium-deficient hydroxyapatite coatings on a Ti6Al4V substrate, the precipitation of a new crystalline apatite occurs. It was also noticed that there was an increase in the Ca/P atomic ratio value from 1.5 (before the immersion in the DMEM medium) to a Ca/P value of around 1.65 (after the immersion in the DMEM medium) [22]. Further, it was noticed that by immersing in a DMEM solution, the dissolution of calcium-deficient hydroxyapatite coatings occurs followed by the precipitation of a new apatite layer [22]. These results make such biomaterials suitable for use in orthopedic or dental applications since they favor the formation of new bone tissue [22].

It is known that Zinc (Zn) ions are one of the significant trace elements present in bone tissue [23]. Zinc ions participate in important bone processes such as bone development and biomineralization [23–25]. Therefore, the Zn incorporation in the hydroxyapatite structure can enhance their bioactivity [23–26].

The point of this study was to evaluate for the first time the new layer formation on the surface of zinc-doped hydroxyapatite–chitosan (ZnHApC) composite coatings after soaking in a biological medium (DMEM). For this purpose, we used techniques such as attenuated total reflection (ATR), Fourier transform infrared (FTIR) spectroscopy, metallographic microscopy (MM), and scanning electron microscopy (SEM). In addition, water contact angle measurements and swelling and adhesion studies were performed. The ZnHApC coatings were developed by vacuum deposition technique, and their physicochemical and biological features before and after soaking in a DMEM medium were presented. The biological assay conducted on ZnHApC was done with the aid of a primary osteoblast cell line. Moreover, antifungal activity against the *Candida albicans* fungal strain was evaluated.

2. Materials and Methods

2.1. Synthesis of Zinc-Doped Hydroxyapatite–Chitosan (ZnHApC) Powders

For the synthesis of zinc-doped hydroxyapatite–chitosan ($Ca_{10-x}Zn_x(PO_4)_6(OH)_2$; x_{Zn} = 0.07; ZnHApC) powders, the protocol described in our previous paper was used [21]. For this objective, during the synthesis, the [Ca + Zn]/P ratio was kept at 1.67 and the pH value was maintained at 11. The obtaining procedure was performed in air. The proper amounts of $Zn(NO_3)_2 \cdot 6H_2O$ (Alfa Aesar, Karlsruhe, Germany) and $Ca(NO_3)_2 \cdot 4H_2O$ (calcium nitrate tetrahydrate; Sigma Aldrich, St. Louis, MO, USA) were dissolved and the obtained solution was slowly added into a solution containing $(NH_4)_2 \cdot HPO_4$ (Alfa Aesar, Karlsruhe, Germany) and chitosan ($C_6H_{11}NO_4$; Sigma Aldrich, St. Louis, MO, USA). The obtained mixture was stirred at 100 °C for 4 h and then centrifugated. Then, the precipitate was redispersed in an aqueous solution under vigorous stirring at 100 °C. Last, the ZnHApC precipitate was dried at 100 °C and used for the vacuum deposition of the ZnHApC composite coatings.

2.2. Deposition of ZnHApC Coatings on Si Substrate

The ZnHApC thin films were deposited on Si substrates. Before the vacuum deposition, the substrate was cleaned several times with acetone and dried in the air at 40 °C. The parameters used for the coating's deposition were described in detail by Predoi et al. [16]. Further, the ZnHApC thin films were soaked in a DMEM medium (Sigma Aldrich, St. Louis, MO, USA) in an incubator (GFL 4010, GFL Gesellschaft für Labortechnik mbH, Burgwedel, Germany) at 37 °C ± 0.5 °C. Initially, 2 sample batches were soaked in DMEM (which was changed daily). The first sample batch was taken out after 7 days (ZnHApC-7D) and the second sample batch after 14 days (ZnHApC-7D). After being taken out from the biological environment, the samples were washed with double-distilled water and placed in a desiccator.

2.3. Physical, Chemical, and Morphological Characterizations

The attenuated total reflection-Fourier transform infrared (ATR-FTIR) spectra were obtained with the aid of a Jasco FTIR-6600 spectrometer (Easton, MD, USA). The spectra were acquired from 450 to 2000 cm^{-1} with a spectral resolution of 4 cm^{-1} averaging 128 scans.

The morphology and EDX compositional studies of ZnHApC powders and coatings were performed using a scanning electron microscope (Hitachi S4500, Hitachi, Tokyo, Japan).

Preliminary assessments of the ZnHApC coatings surface before and after the soaking in the biological medium were obtained using the 10× magnification objective of an inversed trinocular metallographic microscope OX.2153-PLM, (Euromex, Arnhem, The Netherlands). Image J software (Image J 1.51j8) [27] was used for the 3D representation of SEM and metallographic images.

The water contact angle studies were performed under ambient conditions using a contact angle goniometer (DSA30 Kruess GmbH, Hamburg, Germany). For these experiments, the sessile drop technique was used. The contact angle measurements were repeated 3 times for each composite coating. The values of the contact angle ± SD are presented.

Dried ZnHApC, ZnHApC-7D, and ZnHApC-14D coatings were weighted (W_D) before the swelling test. Then the dried coatings were immersed in deionized water. Finally, the samples were taken out of the water after 24 h. The water excess was removed with filter paper and then the samples were weighed again (W_W). The swelling test was repeated 3 times, and the results are presented as mean value ± SD. The swelling percentage was calculated with the following formula:

$$\text{Swelling } (\%) = \frac{W_{W-W_D}}{W_D} \times 100 \quad (1)$$

The adherence of the ZnHApC, ZnHApC-7D, and ZnHApC-14D coatings to the substrate was determined using the tape-pull test. The adhesion tests were performed using the 3M Performance Flatback Tape 2525, having a peel adhesion of 7.5 N/cm.

2.4. Cytotoxicity Assay

The biological properties of the ZnHApC, ZnHApC-7D, and ZnHApC-14D samples were investigated using primary human osteoblast cells, hFOB 1.19. The cells were procured from the upper part of a patient's femur following the protocol described by Gallagher et al. [28]. The *in vitro* biocompatibility study assays were performed as previously reported in detail in [29] and the cell viability of the hFOB 1.19 cells was determined after 24 and 72 h of incubation with the composite layers. The *in vitro* experiments were done in triplicate. The data were reported as mean ± standard deviation (SD). Furthermore, the statistical analysis was performed using the t-test and analysis of variance (ANOVA).

2.5. Antifungal In Vitro Assay

Studies regarding the antifungal activity of the ZnHApC, ZnHApC-7D, and ZnHApC-14D coatings were performed against the fungal strain *Candida albicans* ATCC 10231. The *in vitro* antifungal assays were done according to the experiments described in [30] and the activity of the samples was determined after 24, 48, and 72 h of incubation with the fungal suspensions. All the experiments were performed in triplicate and the data were graphically represented as mean ± SD.

3. Results

ATR-FTIR measurements were used to study the molecular changes that took place before and after the soaking of ZnHApC coatings in DMEM (Figure 1). In Figure 1, the presence of characteristic adsorption bands of HAp can be easily observed. The absorption bands were found at 480, 564, 606, 960, and 1090 cm^{-1} and are ascribed to PO_4^{3-} vibration, and their presence was observed for all studied coatings [21,31]. On the other hand, in the FTIR spectra of ZnHApC-14D (Figure 1c) coatings, the presence of the adsorption bands at 869, 1416, and 1484 cm^{-1}, ascribed to CO_3^{2-} groups, was noticed, which suggests the presence of a carbonated hydroxyapatite layer on the sample's surface [31]. Furthermore, in the region from 1300 until 1500 cm^{-1}, bands that are ascribed to the chitosan structure are present [21,31].

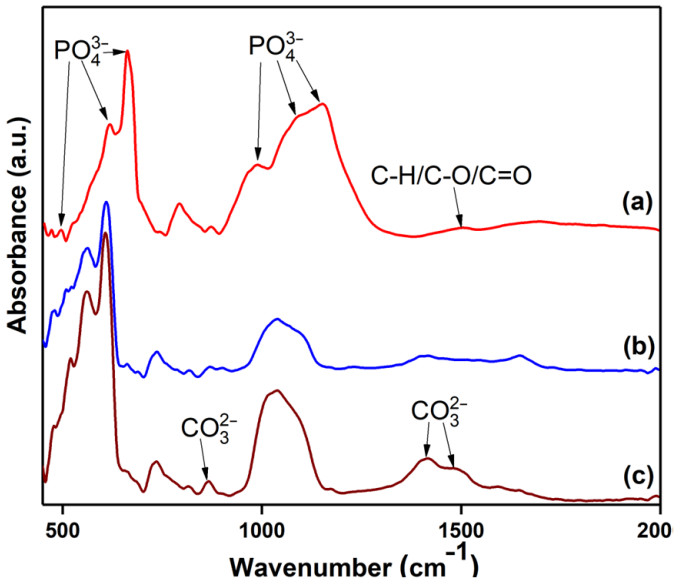

Figure 1. Absorbance ATR-FTIR spectra of ZnHApC (**a**), ZnHApC-7D (**b**), and ZnHApC-14D (**c**) coatings.

According to the studies made by Vladescu A. and collaborators, [32] the presence of carbonate bands in the FTIR spectra suggests the formation of an apatitic layer. Moreover, the presence of carbonate bands in the FTIR spectra underlines the replacement of PO_4^{3-} with CO_3^{2-} functional groups in the HAp structure [31,32].

After the coatings were soaked in DMEM for 7 and 14 days, the increase in adsorption band intensity can be observed. Also, the ZnHApC-14D exhibits more intense peaks ascribed to carbonate groups. The FTIR studies' results underline that samples soaking in DMEM induce some changes in the soaked coatings [31,32].

First, we have conducted SEM and EDX studies on ZnHApC powders and the results are depicted in Figure 2. Close observation of the SEM micrographs reveals that the ZnHApC powders consist mainly of spherical particles with dimensions in the nanometric range. In the collected SEM images, it can also be observed that the nanoparticles are agglomerated.

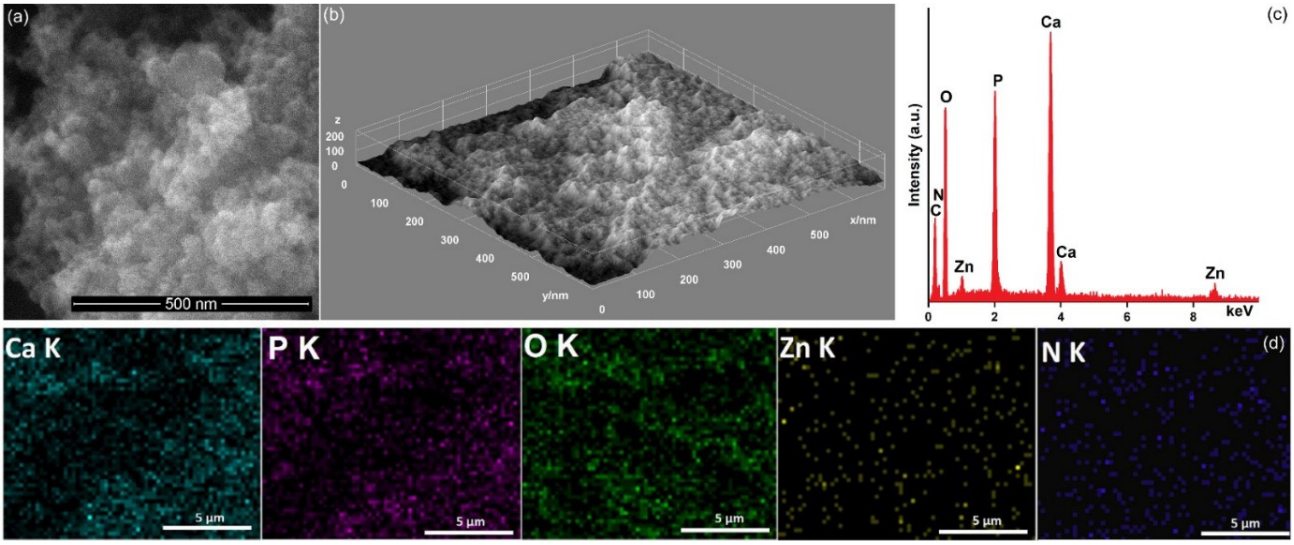

Figure 2. SEM micrographs in 2D and 3D obtained for ZnHApC powders (**a**,**b**). EDX spectra (**c**) and elemental distribution maps ZnHApC powders (**d**).

From the EDX spectra and elemental distribution maps, as depicted in Figure 2, the characteristic peaks of Ca, P, Zn, N, and O are present in the ZnHApC powders. The N line in the EDX spectra arises due to the presence of chitosan in the sample. Also, the surface homogeneity is underlined by the good distribution of the chemical elements in the studied powder. The results of the EDX chemical composition highlighted the purity of the samples.

Figure 3 shows the results of the SEM and EDX studies performed on the ZnHApC coatings before and after soaking (for 7 and 14 days) in DMEM. In the case of ZnHApC, the coatings were inspected before soaking in DMEM. There was the presence of a continuous and uniform layer on the Si substrate surface without the observation of any crack on the coating surface, as indicated by the SEM micrographs (Figure 3a,d).

The formation of a new layer based on calcium and phosphorus (probably a calcium-deficient hydroxyapatite) on the surface of the ZnHApC coatings after 7 and 14 days of exposure to DMEM was proven. The formation of the new layer probably took place by the biomimetic mineralization process as explained by Vranceanu, D.M. and coworkers [6] in their paper entitled: "*In vitro* evaluation of Ag doped hydroxyapatite coatings in acellular media".

Regarding the EDX chemical composition of the analyzed layers, our results indicate the presence of the following chemical elements: calcium, phosphorus, zinc, carbon, nitrogen, and oxygen, in all the samples (Figure 3g–i). Some variation of Ca and P line intensity was observed.

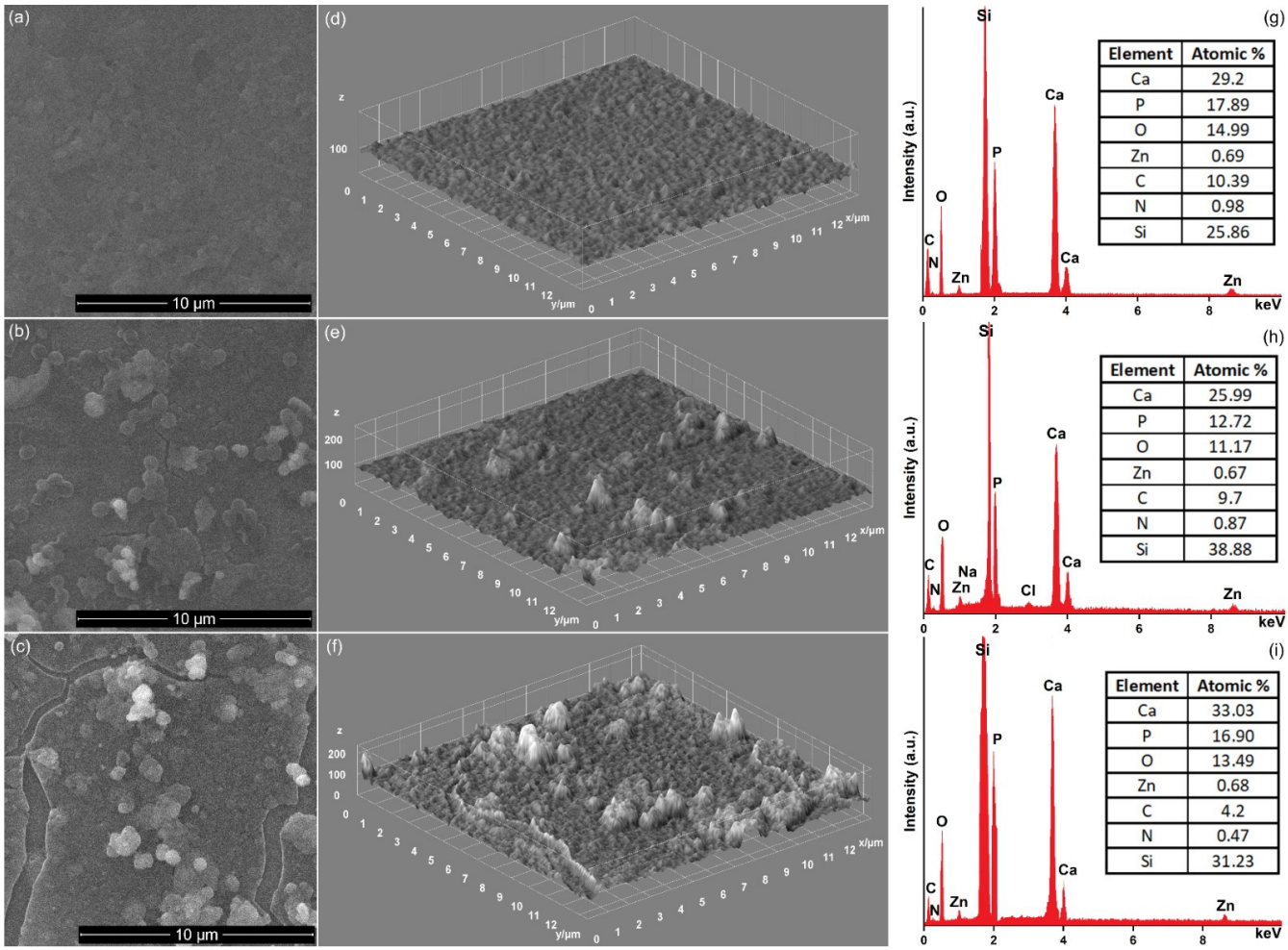

Figure 3. Scanning electron microscopy micrographs (2D and 3D representations) of ZnHApC (**a**,**d**), ZnHApC-7D (**b**,**e**), and ZnHApC-14D(**c**,**f**) coatings and their 3D representations. The energy dispersive X-ray analysis (EDX) spectrum of ZnHApC (**g**), ZnHApC-7D (**h**), and ZnHApC-14D (**i**) coatings.

The results of energy dispersive X-ray spectroscopy (EDS) quantitative analysis (inset of Figure 3g–i) suggest the presence of stoichiometric hydroxyapatite (Ca + Zn)/P = 1.67 in the chitosan matrix in the case of ZnHApC composite coatings. After the soaking in a DMEM medium, the value of the (Ca + Zn)/P ratio varies between 2.095 (for the ZnHApC-7D sample) and 1.99 (for the ZnHApC-14D sample). These values can indicate the formation of a new apatite layer. Our results are in good agreement with the EDX quantitative results previously reported by Vranceanu, D.M. et al. [6].

In the EDX elemental distribution obtained for the ZnHApC-14D coatings, it can be observed that the major constituent are Ca, P, and O. The minor components are represented by Zn, N, and C. Furthermore, the well spatial distribution of both minor and major elements on the ZnHApC-14D coatings surface was observed (Figure 4).

The complementary information regarding the surface characteristics of ZnHApC coatings were achieved by metallographic microscopy (MM) measurements. Figure 5 presents the metallographic image characteristics of the ZnHApC (a and d), ZnHApC-7D (b and e), and ZnHApC-14D (c and h) coatings. In Figure 5, the lack of fissures on the coatings' surface can be observed. The metallographic data sustain the results provided by the SEM studies regarding the formation of a new layer on the ZnHApC subsurface. This is supported by the change in surface morphology of the DMEM-immersed coatings

compared to that of the nonimmersed coating. The SEM features were in agreement with the findings previously reported in the literature [6,32–34].

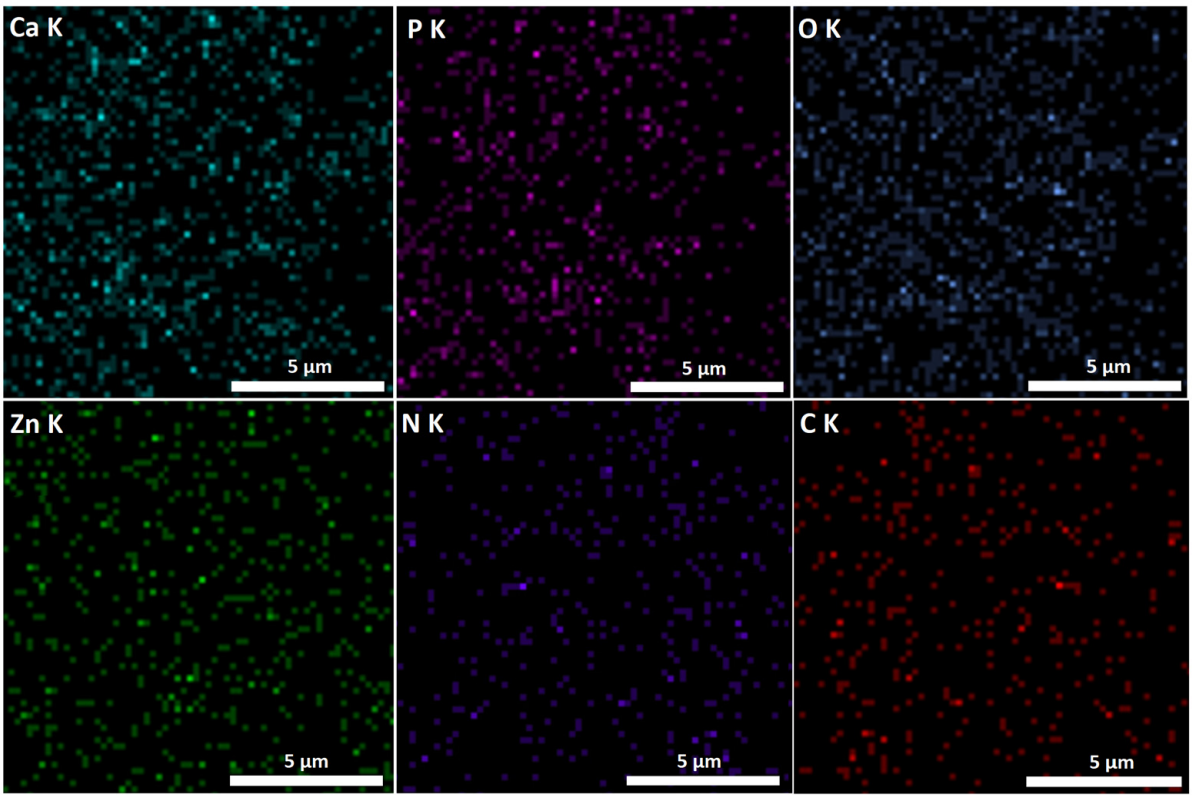

Figure 4. The EDX elemental distributions obtained for ZnHApC-14D coating.

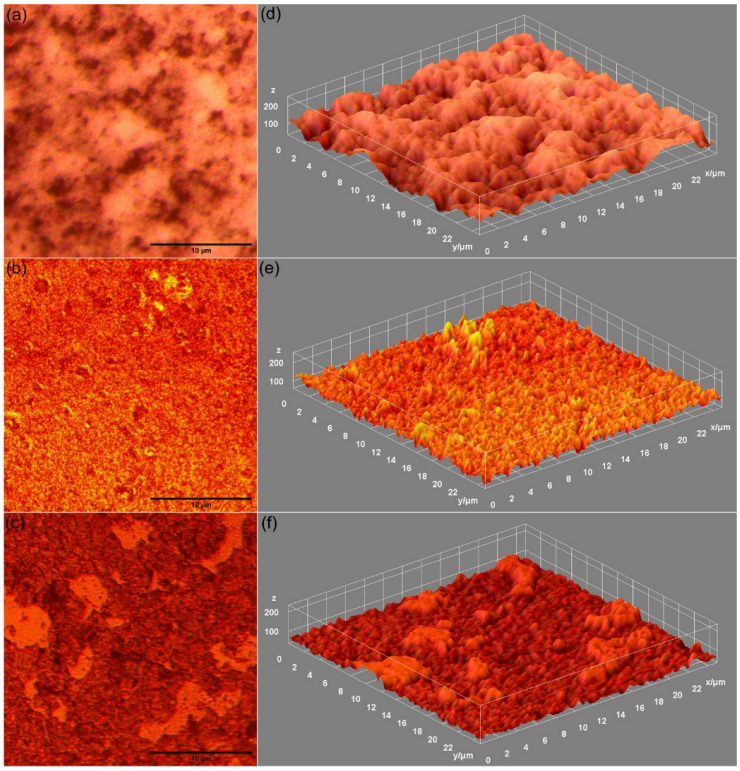

Figure 5. Images in 2D and 3D obtained by metallographic studies on ZnHApC (**a**,**d**), ZnHApC-7D (**b**,**e**), and ZnHApC-14D (**c**,**f**) coatings.

Furthermore, the adherence of ZnHApC, ZnHApC-7D, and ZnHApC-14D on the silicium substrate was investigated using the tape-pull test method. This test is widely known and used for the determination of a coatings' adherence being deemed one of the simplest and fastest-used methods to evaluate a coating's adhesion. In the case of ZnHApC, ZnHApC-7D, and ZnHApC-14D, the experiments highlighted that the scotch tape came off approximately clear, having an insignificant amount of material stuck to it. Therefore, the analysis performed on the coatings suggested that not much of the ZnHApC, ZnHApC-7D, and ZnHApC-14D coatings were actually removed from the substrate. These results emphasized that the ZnHApC, ZnHApC-7D, and ZnHApC-14D coatings presented a good adhesion to the substrate.

The surface properties of ZnHApC t"In 'ilms were evaluated by contact angle measurements and their results are revealed in Table 1. It is known that values higher than 90° indicate a hydrophobic nature of the material surface and values <90° suggest the hydrophilic nature of the sample surface [35].

Table 1. Water contact angle on ZnHApC composite coatings surfaces.

Sample	Contact Angle θ (°)
ZnHApC	57.86 ± 2.75
ZnHApC-7D	48.97 ± 2.3
ZnHApC-14D	42.05 ± 1.5

The obtained value for the contact angle varies between 57.86 ± 2.75° (for ZnHApC) and 42.05 ± 1.5° (for ZnHApC-14D). Therefore, a decrease in the contact angle value that could be attributed to the hydrophilic behavior of apatite could be noticed. More than that, in previous studies, it was shown that the hydrophilic surfaces allowed better cell proliferation and a good growth of apatite in the physiological environment, thus supporting bone growth [36]. In this context, the wettability features of ZnHApC, ZnHApC-7D, and ZnHApC-14D suggest that our samples are hydrophilic which makes them suitable for biomedical applications (orthopedics, dentistry, tissue engineering, etc.) with our results being in concordance with the results previously reported [37].

The water uptake abilities of ZnHApC thin films before and after their soaking in DMEM medium were evaluated by aqueous swelling studies. The results of aqueous swelling studies are presented in Figure 6. Our results suggest that the swelling percentage decreased with the increase in immersion time of the ZnHApC thin films in the DMEM medium.

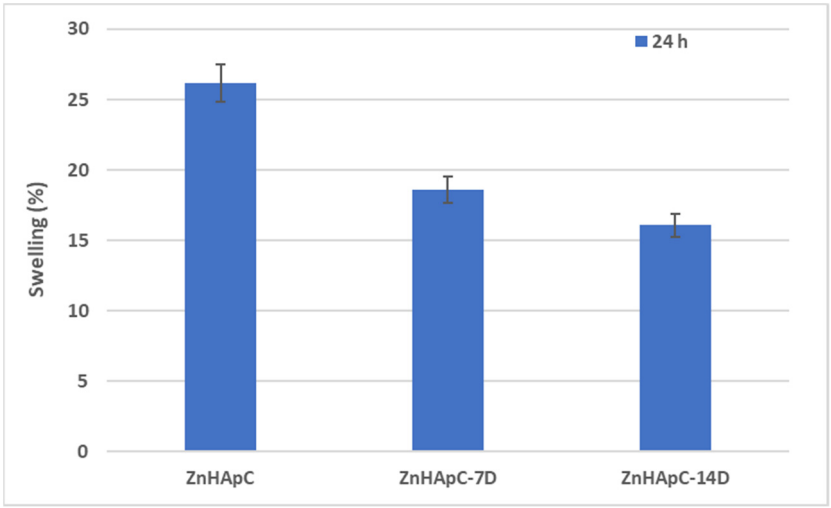

Figure 6. Aqueous swelling percentage of ZnHApC, ZnHApC-7D, and ZnHApC-14D coatings.

The higher swelling percentage was obtained for the ZnHApC thin films (26%), and the lowest value was obtained for the ZnHApC-14D sample (16%). In agreement with the results reported by Bhowmick, A. et al. [38], this behavior may be attributed to the fact that the presence of the apatitic layer on the ZnHApC thin films' surface induced a decrease in the water update capacity. Ponnusamy, S., and coworkers, showed that swelling properties facilitate the use of nutrients from the physiological environment and lead to better adherence [39].

The biocompatibility of the ZnHApC, ZnHApC-7D, and ZnHApC-14D coatings was assessed by *in vitro* experiments using human fetal osteoblast hFOB 1.19 cells. The coatings were incubated for 24 and 72 h with the hFOB 1.19 cell suspensions, and their viability was determined with the aid of the MTT assay. The results obtained from the in vitro MTT tests regarding the cell viability of the hFOB 1.19 incubated with ZnHApC, ZnHApC-7D, and ZnHApC-14D coatings are depicted in Figure 7.

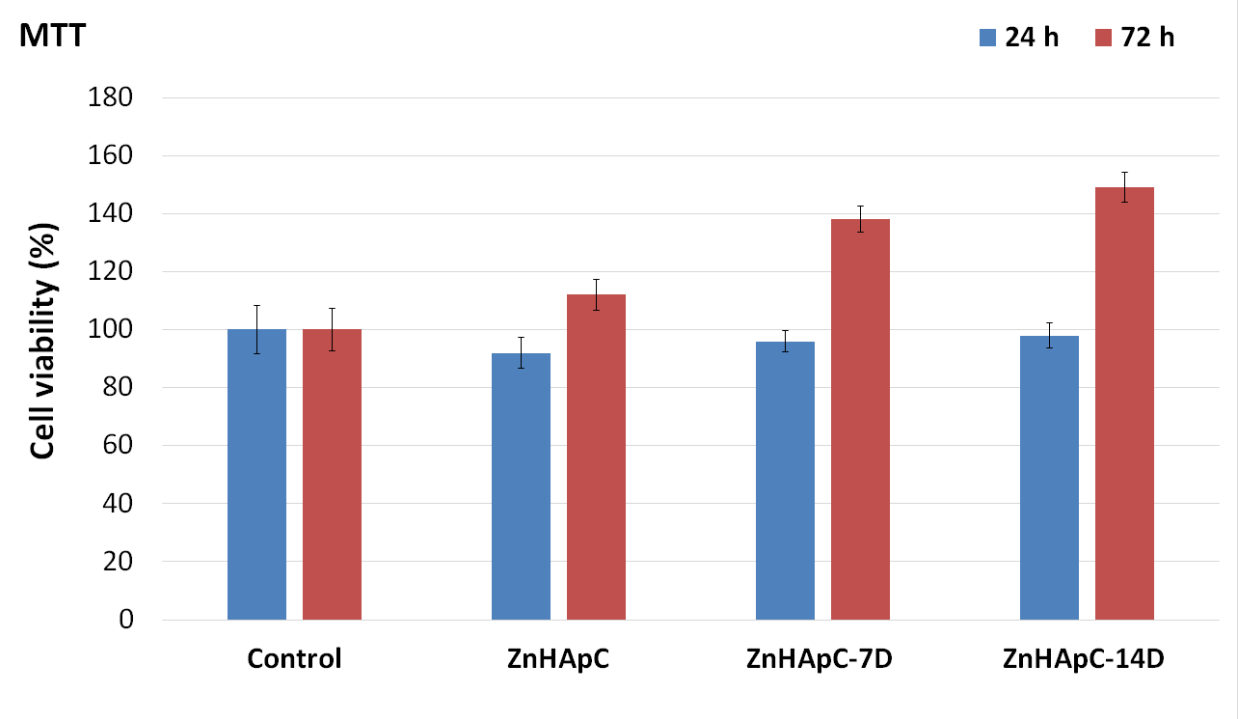

Figure 7. Cell viability of the hFOB 1.19 cells after 24 and 72 h of incubation in the presence of ZnHApC, ZnHApC-7D, and ZnHApC-14D. The results of the experiments are graphically represented as mean ± SD. The data were statistically analyzed using paired and two-sample t-tests for means, with $p \leq 0.05$ accepted as statistically significant.

The experiments were performed in triplicate and the presented data is mean ± SD. The results of the MTT assay determined that all the samples exhibited very good biocompatibility after 24 h of incubation with the hFOB 1.19 cells. However, an increase in cell viability was observed in the case of ZnHApC-7D and ZnHApC-14D compared to the ZnHApC sample. The data suggested that the cell viability increased for the ZnHApC coatings immersed in a DMEM medium. More than that, the results also suggested that the immersion period of the samples in the DMEM medium had an influence on cell viability. In addition, the results of the MTT assays highlighted that all the samples exhibited excellent biocompatibility, being above 92% compared to the control. The obtained results are in concordance with previously reported data regarding hydroxyapatite biocompatibility and its properties of promoting the adherence and proliferation of osteoblast cells [40–50]. Moreover, the cell viability of the hFOB 1.19 cells after 72 h of exposure to ZnHApC, ZnHApC-7D, and ZnHApC-14D coatings presented a significant increase compared to the

control cell culture. Furthermore, the results obtained from the MTT assays after 72 h of exposure of the hFOB 1.19 cells with the composite layers emphasized that all the composite layers presented strong biocompatibility activity and that also helped promote the hFOB 1.19 cells' proliferation and adhesion on the surfaces of the coatings. In addition, the studies demonstrated that the increase observed in the cell viability of hFOB 1.19 cells exposed to ZnHApC-7D and ZnHApC-14D for 72 h was higher than the increase observed in the case of the ZnHApC composite layers. These results could be attributed to the surface changes attained by the ZnHApC composite layers following their immersion in the DMEM medium for 7 and 14 days. More than that, the data also suggested that the increase in cell viability was also influenced by the period of time that the layers were immersed in the DMEM. Therefore, the results highlighted that the immersion in DMEM of the ZnHApC composite layers provided the layers with new surface properties that are responsible for a better proliferation and adhesion of the hFOB 1.19 cell.

Furthermore, the morphology of the hFOB 1.19 cells incubated for 24 and 72 h with the ZnHApC, ZnHApC-7D, and ZnHApC-14D coatings was investigated by microscopy. The results of the morphology investigation of the hFOB 1.19 cells incubated for 24 h with ZnHApC, ZnHApC-7D, and ZnHApC-14D coatings are depicted in Figure 8.

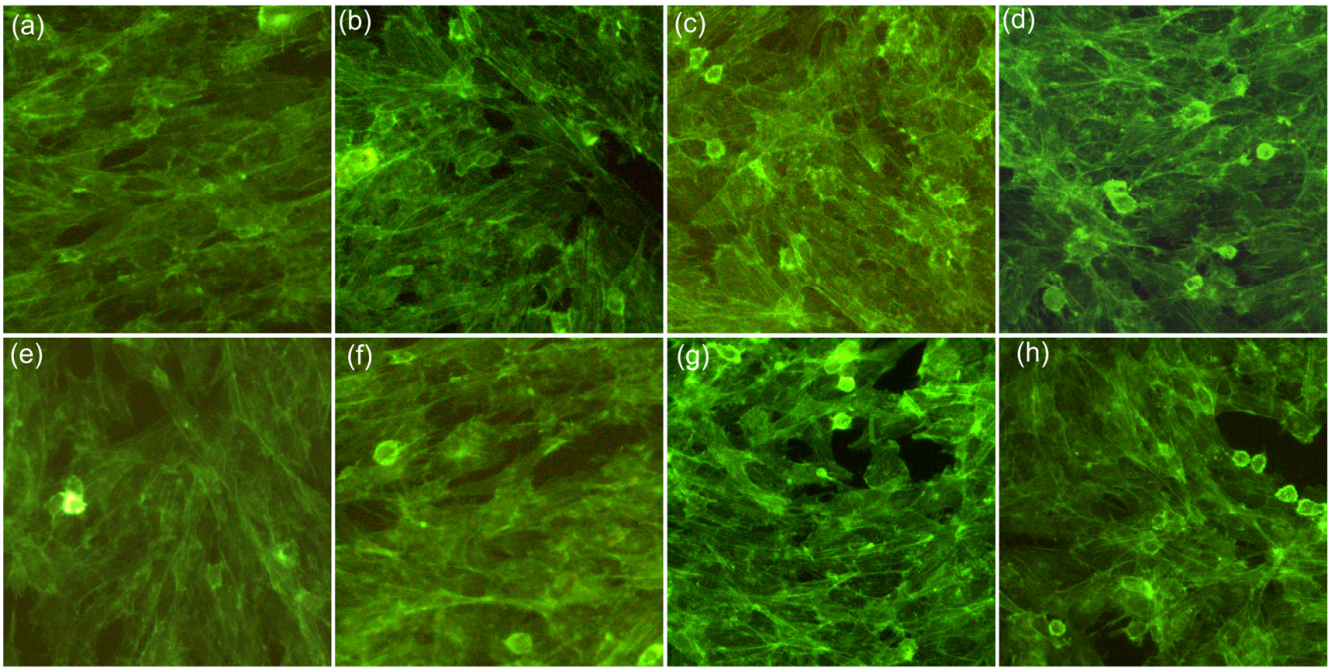

Figure 8. The morphology of hFOB 1.19 cells incubated with ZnHApC (**b**,**f**), ZnHApC-7D (**c**,**g**), and ZnHApC-14D (**d**,**h**) for 24 h (**a**–**d**) and 72 h (**e**–**h**) relative to an untreated hFOB 1.19 cell culture used as control (**a**,**e**).

The images of the hFOB 1.19 cells incubated with ZnHApC, ZnHApC-7D, and ZnHApC-14D coatings highlighted that the cells have adhered on the surface of the ZnHApC, ZnHApC-7D, and ZnHApC-14D coatings and also that the adhered cells exhibit the typical morphology of the hFOB 1.19 cells. Moreover, the visualization of the hFOB 1.19 cells incubated for 24 h with the ZnHApC, ZnHApC-7D, and ZnHApC-14D coatings revealed that coatings did not induce changes to the morphology of the hFOB 1.19 cells. Furthermore, the fluorescence micrographs highlighted that after 72 h of incubation with the ZnHApC composites, the hFOB 1.19 cells adhered and spread until covering almost the entire surface of the composite layers. In addition, the results of the visualization depicted that after 72 h of exposure to the composite layers, the osteoblast cells had the appearance of being organized in confluent layers spread out on the surface of the composite layers. More than that, the results also suggested that the composite layers immersed in a DMEM medium exhib-

ited better biological activity, conferring upon the cells the ability to proliferate and adhere to their surface. These results are in agreement with the MTT assay and emphasized that the immersion in the DMEM medium of the composite layers, as well as the immersion time period, influenced the physicochemical and biological activities of the composite surface, conferring on them enhanced biological properties that lead to better proliferation and adhesion of the cells. Therefore, the data obtained from both the MTT assay, as well as the optical visualization, suggested that the surface of the composite layers affected the metabolic activity of the cells by enhancing their growth. The increase in the hFOB 1.19 cell number was not significant after 24 h of incubation compared to the control cell culture, however, the results showed an abrupt and significant increase ($p < 0.05$) in the number of hFOB 1.19 cells after 72 h of incubation. These results are in good agreement with the results of the quantitative MTT *in vitro* assay and highlighted that ZnHApC, ZnHApC-7D, and ZnHApC-14D coatings have good biocompatibility and could be suitable for being used in biomedical applications.

The results are in good agreement with previously reported studies [51–53] regarding the biological properties of materials based on zinc ions and hydroxyapatite on human osteoblast cells MG-63 [50], mesenchymal stem cells derived from human adipose (MSCs) [44], and MRC-5 fibroblast cells [45]. More than that, in their study, Thian et al. [44] reported that the presence of zinc ions in the structure of hydroxyapatite influenced the bioactivity properties of HAp. In addition to the existing reported data, the results of this study also emphasize that immersion in DMEM of the ZnHApC for 7 and 14 days had an influence on the biological properties of the coatings. Therefore, in the case of ZnHApC-7D and ZnHApC-14D coatings, both the MTT *in vitro* assays, as well as the microscopic visualization, the results depicted that the cell viability, adherence, and proliferation are higher compared to the control cells and ZnHApC coatings. This phenomenon has been explained due to the effect and transformation that appear on the surface of the ZnHApC coatings after being immersed in a DMEM medium. Even though complex studies are still scarce, it has been reported that the increase of the surface charge could also lead to an increase in the wettability and surface energy of various HAp surfaces when using SBF and DMEM mediums [54,55]. Bodhak et al. [50] demonstrated that the increase in the surface energy of HAp obtained by immersion in SBF and DMEM mediums created a better hFOB cell attachment and more points of adhesion between the cells and the surface. On the other hand, Clupper et al. [54] demonstrated that S520 fibers immersed in SBF and DMEM showed promising preliminary results regarding the proliferation, and cell attachment, of osteoblast cells. These preliminary results are promising stepping stones for the future development of novel materials and coatings for biomedical applications that will possess higher bioactive properties and promote faster healing.

In addition, for a better understanding of the complex nature of the influence of the DMEM medium on the biological properties of ZnHApC composite layers, the antifungal properties of ZnHApC, ZnHApC-7D, and ZnHApC-14D coatings were also investigated. For this purpose, due to the fact *Candida albicans* is known as being one of the most opportunistic microorganisms and is also the prevailing cause of fungal infections in humans [56–59], the antifungal properties of the ZnHApC, ZnHApC-7D, and ZnHApC-14D coatings were evaluated against *C. albicans* ATTCC 10231. The composite layers were exposed to the fungal suspensions and their activity against the fungal cell's development was assessed at three different time intervals, 24, 48, and 72 h. The results of the antifungal studies were represented graphically and are depicted in Figure 9.

The results of the *in vitro* studies regarding the antifungal properties of the ZnHApC, ZnHApC-7D, and ZnHApC-14D composite layers depicted that all the investigated samples exhibited good inhibitory effects against the *C. albicans* fungal cells' development. More than that, the data also suggested that the antifungal activity was influenced by both the incubation time as well as the investigated samples. Therefore, the results showed that the antifungal activity of the samples increased with the increase in the incubation time. In addition, the data also suggested that the best inhibitory against the develop-

ment and adherence of *C. albicans* fungal cells on the surface of the composite layers was attributed to the ZnHApC-14D composite layers, therefore implying that the antifungal activity of the ZnHApC composite layers was also influenced by the DMEM immersion. The data obtained in this study is in agreement with previously reported data regarding the antimicrobial properties of materials based on zinc-doped hydroxyapatite in a polymer matrix [26,60–64]. The antifungal properties could be attributed both to the constituent elements of the materials used in the obtaining of the composite layers, as well as to the synergies that could take place between both the constituent elements found in the coatings and the substrate, as well as the synergies between the constituent elements of the composite layers [65,66]. In the case of ZnHApC, ZnHApC-7D, and ZnHApC-14D composite layers, the antifungal properties could be associated first with the presence of zinc ions as well as the presence of chitosan. Over the years, chitosan has been employed in different medical applications due to the fact that is a natural, biodegradable, linear polysaccharide that has been reported to possess both good biocompatibility as well as strong broad-spectrum antimicrobial activity [67–69]. Even though there are numerous papers regarding studies on the antibacterial activity of zinc-doped hydroxyapatite against gram-positive and gram-negative bacterial strains, different efficiencies have been reported [60,61,70–72]. The differences in antimicrobial activity amongst the materials might were reported to be attributed to both particles' physio-chemical characteristics and, especially, to the different surface properties, which can be strongly influenced by the type of material as well as their surface properties.

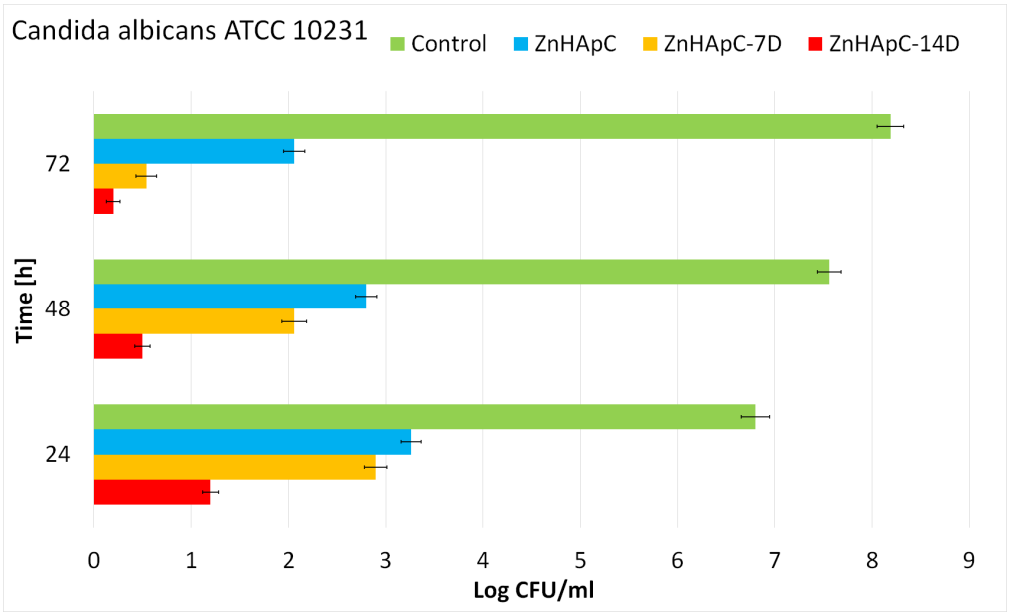

Figure 9. The graphical representation of the antifungal activity of ZnHApC, ZnHApC-7D, and ZnHApC-14D composite layers after 24, 48, and 72 h of exposure to *Candida albicans* ATCC 10231.

The results obtained by the biological assays emphasized that the Immersion in DMEM medium for 7 and 14 days of the ZnHApC composite layers determined changes in the layers' surfaces and granted the layers novel enhanced biological properties that helped promoted the adherence and proliferation of osteoblast cells on their surfaces while inhibiting the development of *C. albicans* fungal cells. In addition, the data also suggested that the immersion time helped improve the biological properties of the ZnHApC composite layers. The results of this study could contribute significantly as leading-edge knowledge for the future development of coatings with enhanced biological properties and antifungal properties for biomedical applications.

4. Conclusions

The main objective of this paper was to develop, by an adapted coprecipitation method, zinc-doped hydroxyapatite–chitosan (ZnHApC) powders. The ZnHApC nanopowders were used for fabrication by the vacuum deposition method of ZnHApC coatings. Then, on the obtained coatings, studies were performed in order to evaluate the formation of a new apatitic layer after their exposure to DMEM (a biological medium) for 7 and 14 days. Thus, FTIR, SEM, EDX, and metallographic studies were carried out. Our findings prove the development of a layer rich in Ca and P that underlines the good mineralization abilities of ZnHApC exposed to a biological medium. The good biocompatibility of ZnHApC, ZnHApC-7D, and ZnHApC-14D was pointed out with the aid of the hFOB 1.19 cell line. Furthermore, the antifungal activity of the ZnHApC, ZnHApC-7D, and ZnHApC-14D composite layers was also assessed against *C. albicans* fungal cells. The results of the biological assays demonstrated that all the samples exhibited good biocompatibility and strong inhibitory effects against the tested fungal cells. In addition, the results also suggested that the biological properties of the ZnHApC composite layers were considerably enhanced due to immersion in the DMEM medium. More than that, the data also emphasized that the biological properties of the layers were also influenced differently according to their immersion time in the DMEM medium. These first results are promising stepping stones for the future development of novel materials and coatings for biomedical applications that will possess higher bioactive properties, promote faster healing, and exhibit antifungal properties.

Author Contributions: Conceptualization, M.M.-H. and D.P.; methodology, D.P.; software, M.V.P.; validation, M.M.-H., D.P. and S.L.I.; formal analysis, M.M.-H.; investigation, M.M.-H., D.P., S.C.C., M.V.P. and S.L.I.; resources, M.M.-H., D.P. and M.V.P.; data curation, M.M.-H.; writing—original draft preparation, D.P., S.C.C., M.V.P. and S.L.I.; writing—review and editing, M.M.-H., D.P., S.C.C., M.V.P. and S.L.I.; visualization, M.M.-H., D.P., S.C.C., M.V.P. and S.L.I.; supervision, M.M.-H., S.L.I. and D.P.; project administration, D.P.; funding acquisition, D.P. All authors have read and agreed to the published version of the manuscript.

Funding: This work was supported by the Romanian Ministry of Research and Innovation through the PN-III-P2-2.1-PED-2019-1375, contract number 331PED/2020. Also, this research was supported by Contract No. T-IS 251801/04.05.2018 and Scientific Research Contract Nr.1/4.06.2020.

Institutional Review Board Statement: Not applicable.

Informed Consent Statement: Not applicable.

Data Availability Statement: Data available on demand from the corresponding author.

Acknowledgments: We would like to thank Rodica V. Ghita for her help with the vacuum deposition of coatings. Also, the authors would like to thank Monica Luminita Badea for assistance with the biological assays.

Conflicts of Interest: The authors declare no conflict of interest. The funders had no role in the design of the study; in the collection, analyses, or interpretation of data; in the writing of the manuscript; or in the decision to publish the results.

References

1. Rohanová, D.; Boccaccini, A.R.; Horkavcová, D.; Bozděchová, P.; Bezdička, P.; Častorálová, M. Is non-buffered DMEM solution a suitable medium for in vitro bioactivity tests? *J. Mater. Chem. B* **2014**, *2*, 5068–5076. [CrossRef]
2. Kokubo, T. Bioactive glass ceramics: Properties and applications. *Biomaterials* **1991**, *12*, 155–163. [CrossRef] [PubMed]
3. Kokubo, T.; Takadama, H. How useful is SBF in predicting in vivo bone bioactivity? *Biomaterials* **2006**, *27*, 2907–2915. [CrossRef] [PubMed]
4. Lee, J.T.; Leng, Y.; Chow, K.L.; Ren, F.; Ge, X.; Wang, K.; Lu, X. Cell culture medium as an alternative to conventional simulated body fluid. *Acta Biomater.* **2011**, *7*, 2615–2622. [CrossRef]
5. Um, S.H.; Chung, Y.W.; Seo, Y.; Seo, H.; Ok, M.R.; Kim, Y.C.; Han, H.S.; Chung, J.J.; Edwards, J.R.; Jeon, H. Robust Hydroxyapatite Coating by Laser-Induced Hydrothermal Synthesis. *Adv. Funct. Mater.* **2020**, *30*, 2005233. [CrossRef]
6. Vranceanu, D.M.; Parau, A.C.; Cotrut, C.M.; Kiss, A.E.; Constantin, L.R.; Braic, V.; Vladescu, A. In vitro evaluation of Ag doped hydroxyapatite coatings in acellular media. *Ceram. Int.* **2019**, *45*, 11050–11061. [CrossRef]

7. Faria, D.; Abreu, C.S.; Buciumeanu, M.; Dourado, N.; Carvalho, O.; Silva, F.S.; Miranda, G. Ti6Al4V laser surface preparation and functionalization using hydroxyapatite for biomedical applications. *J. Biomed. Mater. Res. Part B Appl. Biomater.* **2018**, *106*, 1534–1545. [CrossRef] [PubMed]
8. Arcos, D.; Vallet-Regí, M. Substituted hydroxyapatite coatings of bone implants. *J. Mater. Chem. B* **2020**, *8*, 1781–1800. [CrossRef] [PubMed]
9. Ratnayake, J.T.B.; Mucalo, M.; Dias, G.J. Substituted hydroxyapatites for bone regeneration: A review of current trends. *J. Biomed. Mater. Res. B Appl. Biomater.* **2017**, *105*, 1285–1299. [CrossRef] [PubMed]
10. Boccaccini, A.R.; Keim, S.; Ma, R.; Li, Y.; Zhitomirsky, I. Electrophoretic deposition of biomaterials. *J. R. Soc. Interface* **2010**, *7*, S581–S613. [CrossRef] [PubMed]
11. Kazimierczak, P.; Benko, A.; Nocun, M.; Przekora, A. Novel chitosan/agarose/hydroxyapatite nanocomposite scaffold for bone tissue engineering applications: Comprehensive evaluation of biocompatibility and osteoinductivity with the use of osteoblasts and mesenchymal stem cells. *Int. J. Nanomed.* **2019**, *14*, 6615–6630. [CrossRef] [PubMed]
12. Kazimierczak, P.; Golus, J.; Kolmas, J.; Wojcik, M.; Kolodynska, D.; Przekora, A. Noncytotoxic zinc-doped nanohydroxyapatite-based bone scaffolds with strong bactericidal, bacteriostatic, and antibiofilm activity. *Biomat. Adv.* **2022**, *139*, 213011. [CrossRef]
13. Douglas, L.J. Candida biofilms and their role in infection. *Trends Microbiol.* **2003**, *11*, 30–36. [CrossRef]
14. Ferreira, A.V.; Prado, C.G.; Carvalho, R.R.; Dias, K.S.T.; Dias, A.L.T. Candida albicans and non-C. albicans Candida species: Comparison of biofilm production and metabolic activity in biofilms, and putative virulence properties of isolates from hospital environments and infections. *Mycopathologia* **2013**, *175*, 265–272. [CrossRef] [PubMed]
15. Pierce, G.E. Pseudomonas aeruginosa, Candida albicans, and device-related nosocomial infections: Implications, trends, and potential approaches for control. *J. Ind. Microbiol. Biotechnol.* **2005**, *32*, 309–318. [CrossRef] [PubMed]
16. Rajesh, P.; Mohan, N.; Yokogawa, Y.; Varma, H. Pulsed laser deposition of hydroxyapatite on nanostructured titanium towards drug eluting implants. *Mater. Sci. Eng. C* **2013**, *33*, 2899–2904. [CrossRef] [PubMed]
17. Negroiu, G.; Piticescu, R.M.; Chitanu, G.C.; Mihailescu, I.N.; Zdrentu, L.; Miroiu, M. Biocompatibility evaluation of a novel hydroxyapatite-polymer coating for medical implants (in vitro tests). *J. Mater. Sci. Mater. Med.* **2008**, *19*, 1537–1544. [CrossRef] [PubMed]
18. Snyders, R.; Bousser, E.; Music, D.; Jensen, J.; Hocquet, S.; Schneider, J.M. Influence of the chemical composition on the phase constitution and the elastic properties of RF-sputtered hydroxyapatite coatings. *Plasma Process. Polym.* **2008**, *5*, 168–174. [CrossRef]
19. Hench, L.L.; West, J.K. The sol-gel process. *Chem. Rev.* **1990**, *90*, 33–72. [CrossRef]
20. Qiu, D.; Yang, L.; Yin, Y.; Wang, A. Preparation and characterization of hydroxyapatite/titania composite coating on NiTi alloy by electrochemical deposition. *Surf. Coat. Technol.* **2011**, *205*, 3280. [CrossRef]
21. Predoi, D.; Ciobanu, C.S.; Iconaru, S.L.; Raaen, S.; Badea, M.L.; Rokosz, K. Physicochemical and Biological Evaluation of Chitosan-Coated Magnesium-Doped Hydroxyapatite Composite Layers Obtained by Vacuum Deposition. *Coatings* **2022**, *12*, 702. [CrossRef]
22. Dumelie, N.; Benhayoune, H.; Richard, D.; Laurent-Maquin, D.; Balossier, G. In vitro precipitation of electrodeposited calcium-deficient hydroxyapatite coatings on Ti6Al4V substrate. *Mater. Charact.* **2008**, *59*, 129–133. [CrossRef]
23. Wu, S.; Ma, S.; Zhang, C.; Cao, G.; Wu, D.; Gao, C.; Lakshmanan, S. Cryogel biocomposite containing chitosan-gelatin/cerium–zinc doped hydroxyapatite for bone tissue engineering. *Saudi J. Biol. Sci.* **2020**, *27*, 2638–2644. [CrossRef]
24. Yamaguchi, M. Role of nutritional zinc in the prevention of osteoporosis. *Mol. Cell. Biochem.* **2010**, *338*, 241–254. [CrossRef] [PubMed]
25. Huang, Y.; Zhang, X.; Mao, H.; Li, T.; Zhao, R.; Yan, Y.; Pang, X. Osteoblastic cell responses and antibacterial efficacy of Cu/Zn co-substituted hydroxyapatite coatings on pure titanium using electrodeposition method. *RSC Adv.* **2015**, *5*, 17076–17086. [CrossRef]
26. Predoi, D.; Iconaru, S.L.; Predoi, M.V. Fabrication of Silver- and Zinc-Doped Hydroxyapatite Coatings for Enhancing Antimicrobial Effect. *Coatings* **2020**, *10*, 905. [CrossRef]
27. ImageJ. Available online: http://imagej.nih.gov/ij (accessed on 20 November 2022).
28. Gallagher, A.J.; Gundle, R.; Beresford, N.J. Isolation and culture of bone forming cells (osteoblasts) from human bone. *Hum. Cell Cult. Protoc.* **1996**, *2*, 233–263. [CrossRef]
29. Predoi, D.; Iconaru, S.L.; Predoi, M.V. Bioceramic Layers with Antifungal Properties. *Coatings* **2018**, *8*, 276. [CrossRef]
30. Chen, J.; Nan, K.; Yin, S.; Wang, Y.; Wu, T.; Zhang, Q. Characterization and biocompatibility of nanohybrid scaffold prepared via in situ crystallization of hydroxyapatite in chitosan matrix. *Colloids Surf. B.* **2010**, *81*, 640–647. [CrossRef]
31. Iconaru, S.L.; Ciobanu, C.S.; Predoi, G.; Rokosz, K.; Chifiriuc, M.C.; Bleotu, C.; Stanciu, G.; Hristu, R.; Raaen, S.; Raita, S.M.; et al. Biological and Physico-Chemical Properties of Composite Layers Based on Magnesium-Doped Hydroxyapatite in Chitosan Matrix. *Micromachines* **2022**, *13*, 1574. [CrossRef] [PubMed]
32. Vlădescu, A.; Pârâu, A.; Pană, I.; Cotruț, C.M.; Constantin, L.R.; Braic, V.; Vrânceanu, D.M. In Vitro Activity Assays of Sputtered HAp Coatings with SiC Addition in Various Simulated Biological Fluids. *Coatings* **2019**, *9*, 389. [CrossRef]
33. Stojanović, S.; Mitić, Ž.; Miljković, M.; Rajković, J.; Trajanović, M.; Najman, S. SEM-EDX analysis of BIO-OSS®granules after incubation in cell culture medium. In Proceedings of the III Advanced Ceramics and Applications Conference, 29 September 2014; Atlantis Press: Paris, France, 2016; pp. 259–264. [CrossRef]

34. John, Ł.; Bałtrukiewicz, M.; Sobota, P.; Brykner, R.; Cwynar-Zając, Ł.; Dzięgiel, P. Non-cytotoxic organic–inorganic hybrid bioscaffolds: An efficient bedding for rapid growth of bone-like apatite and cell proliferation. *Mater. Sci. Eng. C* **2012**, *32*, 1849–1858. [CrossRef] [PubMed]
35. Silverstein, R.M.; Webster, F.X.; Kiemle, D.; Bryce, D.L. *Spectrometric Identification of Organic Compounds*, 8th ed.; John Wiley & Sons: Hoboken, NJ, USA, 2014.
36. Law, K.Y. Definitions for Hydrophilicity, Hydrophobicity, and Superhydrophobicity: Getting the Basics Right. *J. Phys. Chem. Lett.* **2014**, *5*, 686–688. [CrossRef]
37. Ansari, Z.; Kalantar, M.; Soriente, A.; Fasolino, I.; Kharaziha, M.; Ambrosio, L.; Raucci, M.G. In-Situ Synthesis and Characterization of Chitosan/Hydroxyapatite Nanocomposite Coatings to Improve the Bioactive Properties of Ti6Al4V Substrates. *Materials* **2020**, *13*, 3772. [CrossRef] [PubMed]
38. Saleem, O.; Wahaj, M.; Akhtar, M.A.; Ur Rehman, M.A. Fabrication and Characterization of Ag-Sr-Substituted Hydroxyapatite/Chitosan Coatings Deposited via Electrophoretic Deposition: A Design of Experiment Study. *ACS Omega* **2020**, *5*, 22984–22992. [CrossRef] [PubMed]
39. Bhowmick, A.; Pramanik, N.; Mitra, T.; Gnanamani, A.; Das, M.; Kundu, P.P. Mechanical and biological investigations of chitosan–polyvinyl alcohol based ZrO_2 doped porous hybrid composites for bone tissue engineering applications. *New J. Chem.* **2017**, *41*, 7524–7530. [CrossRef]
40. Ponnusamy, S.; Subramani, R.; Elangomannan, S.; Louis, K.; Periasamy, M.; Dhanaraj, G. Novel Strategy for Gallium-Substituted Hydroxyapatite/Pergularia daemia Fiber Extract/Poly(N-vinylcarbazole) Biocomposite Coating on Titanium for Biomedical Applications. *ACS Omega* **2021**, *6*, 22537–22550. [CrossRef] [PubMed]
41. Thian, E.S.; Ahmad, Z.; Huang, J.; Edirisinghe, M.J.; Jayasinghe, S.N.; Ireland, D.C.; Brooks, R.A.; Rushton, N.; Bonfield, W.; Best, S.M. The role of surface wettability and surface charge of electrosprayed nanoapatites on the behaviour of osteoblasts. *Acta Biomater.* **2010**, *6*, 750–755. [CrossRef]
42. Predoi, D.; Iconaru, S.L.; Deniaud, A.; Chevallet, M.; Michaud-Soret, I.; Buton, N.; Prodan, A.M. Textural, Structural and Biological Evaluation of Hydroxyapatite Doped with Zinc at Low Concentrations. *Materials* **2017**, *10*, 229. [CrossRef] [PubMed]
43. Battistoni, C.; Casaletto, M.P.; Ingo, G.M.; Kaciulis, S.; Mattogno, G.; Pandolfi, L. Surface characterization of biocompatible hydroxyapatite coatings. *Surf. Interface Anal.* **2000**, *29*, 773–781. [CrossRef]
44. Thian, E.S.; Konishi, T.; Kawanobe, Y.; Lim, P.N.; Choong, C.; Ho, B.; Aizawa, M. Zinc-substituted hydroxyapatite: A biomaterial with enhanced bioactivity and antibacterial properties. *J. Mater. Sci. Mater. Med.* **2013**, *24*, 437–445. [CrossRef] [PubMed]
45. Radovanović, Ž.; Veljović, D.; Jokić, B.; Dimitrijević, S.; Bogdanović, G.; Kojić, V.; Petrović, R.; Janaćković, D. Biocompatibility and antimicrobial activity of zinc(II)-doped hydroxyapatite, synthesized by a hydrothermal method. *J. Serb. Chem. Soc.* **2012**, *77*, 1787–1798. [CrossRef]
46. Ren, F.; Xin, R.; Ge, X.; Leng, Y. Characterization and structural analysis of zinc-substituted hydroxyapatites. *Acta Biomater.* **2009**, *5*, 3141–3149. [CrossRef] [PubMed]
47. Ben-Nissan, B.; Choi, A.H. Sol–gel production of bioactive nano-coatings for medical applications. Part 1: An introduction. *Nanomedicine* **2006**, *1*, 311–319. [CrossRef] [PubMed]
48. Fahami, A.; Beall, G.W.; Betancourt, T. Synthesis, bioactivity and zeta potential investigations of chlorine and fluorine substituted hydroxyapatite. *Mater. Sci. Eng. C Mater. Biol. Appl.* **2016**, *59*, 78–85. [CrossRef]
49. Zhang, J. Biocompatibility and anti-bacterial activity of Zn-containing HA/TiO2 hybrid coatings on Ti substrate. *J. Hard. Tissue Biol.* **2013**, *22*, 311–318. [CrossRef]
50. Tank, K.P.; Chudasama, K.S.; Thaker, V.S.; Joshi, M.J. Pure and zinc doped nano-hydroxyapatite: Synthesis, characterization, antimicrobial and hemolytic studies. *J. Cryst. Growth* **2014**, *401*, 474–479. [CrossRef]
51. Bodhak, S.; Bose, S.; Bandyopadhyay, A. Role of surface charge and wettability on early stage mineralization and bone cell–materials interactions of polarized hydroxyapatite. *Acta Biomater.* **2009**, *5*, 2178–2188. [CrossRef]
52. Korbut, A.; Włodarczyk, M.; Rudnicka, K.; Szwed, A.; Płociński, P.; Biernat, M.; Tymowicz-Grzyb, P.; Michalska, M.; Karska, N.; Rodziewicz-Motowidło, S.; et al. Three Component Composite Scaffolds Based on PCL, Hydroxyapatite, and L-Lysine Obtained in TIPS-SL: Bioactive Material for Bone Tissue Engineering. *Int. J. Mol. Sci.* **2021**, *22*, 13589. [CrossRef]
53. du Pree, I.; Richter, W.; van Papendorp, D.; Joubert, A. hFOB 1.19 osteoblast cells grown on a biomimetic biphasic nanoscaffold: An in vitro evaluation for possible bone tissue engineering. *Biomed. Res.* **2018**, *29*, 2442–2448.
54. Kazimierczak, P.; Vivcharenko, V.; Truszkiewicz, W.; Wójcik, M.; Przekora, A. Osteoblasts response to Novel chitosan/agarose/hydroxyapatite bone scaffold—Studies on mc3t3-e1 and hfob 1.19 cellular models. *Eng. Biomater.* **2019**, *15*, 24–29.
55. Clupper, D.C.; Gough, J.E.; Hall, M.M.; Clare, A.G.; LaCourse, W.C.; Hench, L.L. In vitro bioactivity of S520 glass fibers and initial assessment of osteoblast attachment. *J. Biomed. Mater. Res. A* **2003**, *67*, 285–294. [CrossRef] [PubMed]
56. Bedi, R.S.; Chow, G.; Wang, J.; Zanello, L.; Yan, Y.S. Bioactive materials for regenerative medicine: Zeolite-hydroxyapatite bone mimetic coatings. *Adv. Eng. Mater.* **2012**, *14*, 200–206. [CrossRef]
57. Papon, N.; Courdavault, V.; Clastre, M.; Bennett, R.J. Emerging and emerged pathogenic Candida species: Beyond the Candida albicans paradigm. *PLoS Pathog* **2013**, *9*, e1003550. [CrossRef] [PubMed]
58. Martin, M.V. The use of fluconazole and itraconazole in the treatment of Candida albicans infections: A review. *J. Antimicrob. Chemoth.* **1999**, *44*, 429–437. [CrossRef]

59. Weiner, L.M.; Webb, A.K.; Limbago, B.; Dudeck, M.A.; Patel, J.; Kallen, A.J.; Edwards, J.R.; Sievert, D.M. Antimicrobial-resistant pathogens associated with health care associated infec-tions: Summary of data reported to the National Healthcare Safety Network at the Centers for Disease Control and Prevention, 2011–2014. *Infect. Cont. Hosp. Epidemol.* **2016**, *37*, 1288–1301. [CrossRef]
60. Kullberg, B.J.; Arendrup, M.C. Invasive candidiasis. *N. Engl. J. Med.* **2015**, *373*, 1445–1456. [CrossRef]
61. Predoi, D.; Iconaru, S.L.; Predoi, M.V. Dextran-Coated Zinc-Doped Hydroxyapatite for Biomedical Applications. *Polymers* **2019**, *11*, 886. [CrossRef]
62. Predoi, D.; Iconaru, S.L.; Predoi, M.V.; Buton, N.; Motelica-Heino, M. Zinc Doped Hydroxyapatite Thin Films Prepared by Sol–Gel Spin Coating Procedure. *Coatings* **2019**, *9*, 156. [CrossRef]
63. Maleki-Ghaleh, H.; Siadati, M.H.; Fallah, A.; Koc, B.; Kavanlouei, M.; Khademi-Azandehi, P.; Moradpur-Tari, E.; Omidi, Y.; Barar, J.; Beygi-Khosrowshahi, Y.; et al. Antibacterial and Cellular Behaviors of Novel Zinc-Doped Hydroxyapatite/Graphene Nanocomposite for Bone Tissue Engineering. *Int. J. Mol. Sci.* **2021**, *22*, 9564. [CrossRef]
64. Okada, M.; Oshita, M.; Kataoka, M.; Azuma, Y.; Furuzono, T. Shareability of antibacterial and osteoblastic-proliferation activities of zinc-doped hydroxyapatite nanoparticles in vitro. *J. Biomed. Mater. Res.* **2022**, *110*, 799–805. [CrossRef] [PubMed]
65. Phatai, P.; Prachumrak, N.; Kamonwannasit, S.; Kamcharoen, A.; Roschat, W.; Phewphong, S.; Futalan, C.M.; Khemthong, P.; Butburee, T.; Youngjan, S.; et al. Zinc-Silver Doped Mesoporous Hydroxyapatite Synthesized via Ultrasonic in Combination with Sol-Gel Method for Increased Antibacterial Activity. *Sustainability* **2022**, *14*, 11756. [CrossRef]
66. Iconaru, S.L.; Predoi, M.V.; Motelica-Heino, M.; Predoi, D.; Buton, N.; Megier, C.; Stan, G.E. Dextran-Thyme Magnesium-Doped Hydroxyapatite Composite Antimicrobial Coatings. *Coatings* **2020**, *10*, 57. [CrossRef]
67. Predoi, D.; Ciobanu, C.S.; Iconaru, S.L.; Predoi, S.A.; Chifiriuc, M.C.; Raaen, S.; Badea, M.L.; Rokosz, K. Impact of Gamma Irradiation on the Properties of Magnesium-Doped Hydroxyapatite in Chitosan Matrix. *Materials* **2022**, *15*, 5372. [CrossRef] [PubMed]
68. Cheung, R.C.; Ng, T.B.; Wong, J.H.; Chan, W.Y. Chitosan: An update on potential biomedical and pharmaceutical applica-tions. *Mar. Drugs* **2015**, *13*, 5156–5186. [CrossRef]
69. Pena, A.; Sanchez, N.S.; Calahorra, M. Effects of chitosan on Candida albicans: Conditions for its antifungal activity. *Biomed. Res. Int.* **2013**, *2013*, 527549. [CrossRef]
70. Sudarshan, N.R.; Hoover, D.G.; Knorr, D. Antibacterial action of chitosan. *Food Biotechnol.* **1992**, *6*, 257–272. [CrossRef]
71. Ofudje, E.A.; Adeogun, A.I.; Idowu, M.A.; Kareem, S.O. Synthesis and characterization of Zn-Doped hydroxyapatite: Scaffold application, antibacterial and bioactivity studies. *Heliyon* **2019**, *5*, e01716 31. [CrossRef]
72. de Lima, C.O.; de Oliveira, A.L.M.; Chantelle, L.; Silva Filho, E.C.; Jaber, M.; Fonseca, M.G. Zn-doped mesoporous hydroxyapatites and their antimicrobial properties. *Colloids Surf. B* **2021**, *198*, 111471. [CrossRef]

Disclaimer/Publisher's Note: The statements, opinions and data contained in all publications are solely those of the individual author(s) and contributor(s) and not of MDPI and/or the editor(s). MDPI and/or the editor(s) disclaim responsibility for any injury to people or property resulting from any ideas, methods, instructions or products referred to in the content.